ELSEVIER

Journal of Alloys and Compounds 317–318 (2001) 532–536

Journal of ALLOYS AND COMPOUNDS

www.elsevier.com/locate/jallcom

Thermodynamic investigation of samarium–nickel alloys

G. Borzone, N. Parodi, R. Raggio, R. Ferro*

Dipartimento di Chimica e Chimica Industriale, Sezione di Chimica Inorganica e Metallurgia, Via Dodecaneso 31, Università di Genova,
I-16146 Genoa, Italy

Abstract

The enthalpies of formation of the Sm–Ni solid alloys at 300 K were determined by direct calorimetry using two different calorimetric apparatus. The characterization of the samples was performed using metallographic and X-ray diffraction analyses. The values of $\Delta_f H°$ (kJ/mol of atoms) for the following compounds were obtained for the formation in the solid state at 300 K: Sm_3Ni: -21.5 ± 2; SmNi: -33.0 ± 1; $SmNi_2$: -36.0 ± 1. The results are discussed and compared with those of other similar rare earth–nickel compounds.

Keywords: Thermochemistry; Formation enthalpy; Rare earth–nickel alloys; Thermodynamic properties; Calorimetry

---

1. Introduction

The intermetallic compounds formed by the rare earth elements (R) and nickel are of particular interest regarding the reversible absorption of a large quantity of hydrogen gas at room temperature and nearly atmospheric pressure. In particular, the exceptional hydriding properties of $LaNi_5$ and $LaNi_5$-based alloys are widely known. Therefore, these alloys are considered for hydrogen storage purposes (hydride heat pumps, Ni–MH rechargeable batteries, etc.) [1]. Thermodynamic and thermochemical data can be very useful for alloying design and processing. As far as the enthalpies of formation are concerned, some data are available for different R–Ni systems, especially in the Ni-rich region. In recent years, a research programme has been set up in our laboratory to study the thermochemistry of R–Ni binary and ternary alloys [2–4].

In the present study the results obtained in a thermodynamic investigation of the Sm–Ni alloys in the 25.0–74.0 at.% Ni region are reported.

2. Literature data on the Sm–Ni system

2.1. Phase diagram and thermodynamic properties of the Sm–Ni alloys

The Sm–Ni phase diagram was previously investigated by Pan and Cheng [5] who also published a revised assessment [6]. The existence of eight intermediate phases was observed: SmNi and $SmNi_5$ which melt congruently at 1079°C and 1430°C, respectively and Sm_3Ni, $SmNi_2$, $SmNi_3$, Sm_2Ni_7, Sm_5Ni_{19} and Sm_2Ni_{17} which form by a peritectic reaction. Three eutectic reactions were observed: $L\rightarrow Sm_3Ni+SmNi$ (at 570°C and 32 at.%Ni), $L\rightarrow SmNi+SmNi_2$ (at 809°C and 53.5 at.%Ni) and $L\rightarrow Sm_2Ni_{17}+Ni$ (at 1280°C and 94 at.%Ni).

The solid solubility of samarium in nickel at 980–1050°C was determined to be about 0.48 mass%, by annealing diffusion couples at 1050° and 980°C for 72*h* and 120*h*, respectively [7]. The Sm-rich portion of the Sm–Ni diagram is still not completely determined.

The enthalpies of formation of $SmNi_2$, $SmNi_3$ and Sm_2Ni_7 [8] and of $SmNi_2$ by [9] have been evaluated and that of $SmNi_5$ determined by Al solution calorimetry [10] and by direct synthesis calorimetry at 1473 K [11]. The standard enthalpies of mixing have been measured for several R–Ni alloys [12], but no data are available for the Sm–Ni system.

The data estimated by Shilov [8] and measured by Pasturel et al. [10] together with the experimental data on the phase diagram have been used for a thermodynamic assessment of the Sm–Ni system by means of the CALPHAD technique [13]. In this optimization, the strongly asymmetric and thermodynamically unlikely liquidus trend around the congruent melting point of SmNi previously suggested, have been discussed.

The calculated phase diagram, which is reported in Fig. 1, agrees well with the invariant equilibrium temperatures

---

*Corresponding author. Tel.: +39-010-353-6149/6161; fax: +39-010-362-5051.

E-mail address: ferro@chimica.unige.it (R. Ferro).

0925-8388/01/$ – see front matter
PII: S0925-8388(00)01382-7

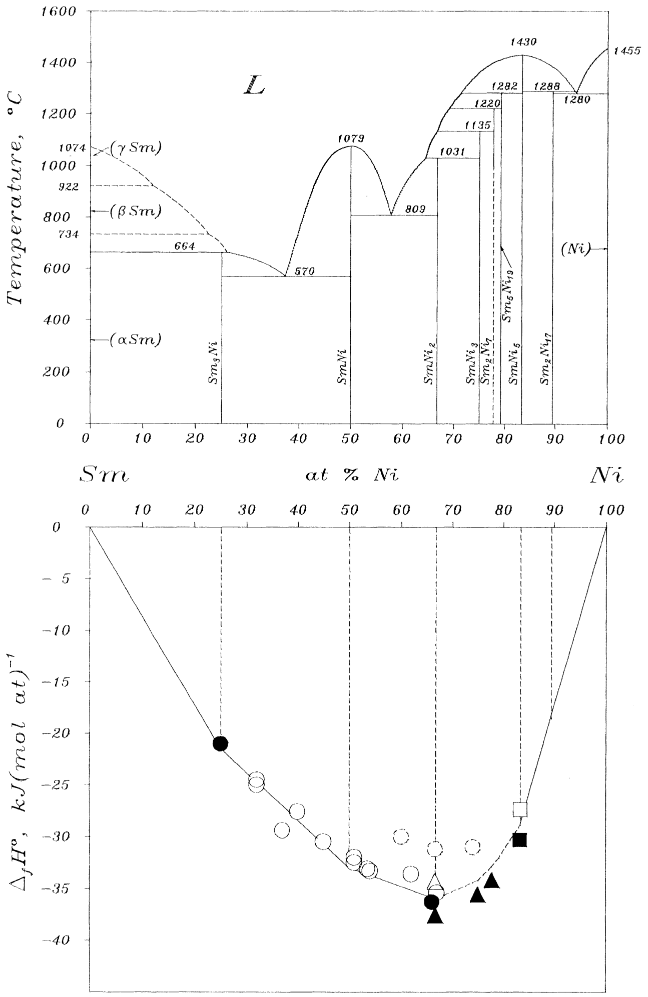

Fig. 1. Sm–Ni system. The phase diagram as assessed by Su et al. [13] is shown. For the invariant reactions, the experimental temperatures obtained by Pan et al. [5,6] are reported (see text). In the lower part of the figure, the experimental values of the $\Delta_f H°$ of the solid alloys are reported. ●, t.w. aneroid calorimeter; ○, t.w. high temperature calorimeter (dotted points refer to samples resulting in an incomplete reaction); △, value estimated by [9]; ▲, values estimated by [8]; □, high temperature calorimetry [11]; ■, Al sol. calorimetry [10]).

obtained by Pan [5]. (Notice however that, in the paper by Su et al., the authors report the calculated phase diagram in comparison with several experimental points ascribed to Pan et al. which, at least partially, seem different from those reported in the original paper by [5]). Small modifications in the Sm-rich eutectic reaction compositions (37.4 instead of 32 at.%Ni and 57.8 instead of 53.5 at.%Ni) have been proposed. In their work, however, Su et al. [13] pointed out that their description of the phase equilibria should be refined. More phase diagram (thermal analysis data) and thermodynamics experimental data are necessary.

In this paper a contribution is given to the formation thermodynamics.

2.2. Crystal structures

The crystal structures and lattice parameters of the Sm–Ni alloys are listed in Table 1. As for the $SmNi_2$ phase, electrical resistivity, thermal expansion and temperature-dependent X-ray diffraction measurements carried out by Gratz et al. on $R_{1-x}Ni_2$ compounds (R=Y, Sm, Gd and Tb) for $0<x<0.05$ gave mutually consistent evidence for structural phase transition [22]. A temperature of 550 K was suggested for the transition from the cubic (high temperature) Laves phase to a low temperature cubic superstructure, with regular vacancies on the rare earth sites and a double lattice parameter. A similar stoichiometry and structure was previously suggested [29] for $LaNi_2$, for which, however, a tetragonal structure was proposed by Gschneidner et al. [30] with $a_t=a_c$, $c_t=2a_c$ (a_c=unit cell edge of the simple Laves phase).

The Sm_5Ni_{19} structure was studied by Takeda et al. [25]. Six polytype structures (2H, 3R, 4H, 6H, 9R and 12R) were found and analysed by high resolution transmission electron microscopy and electron diffraction. Their structures have been described as stacking sequences of Laves phase type layers and $CaCu_5$ type layers. It is not certain whether the four polytypes 4H, 6H, 9R and 12R are stable or metastable phases formed during the phase transformation from 2H and 3R.

Polytytpe structures have also been described for Sm_2Ni_7 [31].

3. Experimental

The alloys were prepared from the elements with a purity of 99.9 (Sm) and 99.99 mass% (Ni), respectively in the 25.0–74.0 at.%Ni composition range.

A number of alloys of selected composition were prepared by sealing appropriate amounts of the elements in tantalum crucibles. The crucibles were induction heated in a vacuum tube furnace under argon atmosphere and subjected to appropriate thermal treatments chosen on the basis of the phase diagram. These alloys were prepared as 'reference' alloys against those prepared in the calorimeter.

The enthalpy of formation measurements were carried out by using two different types of calorimeters built in our laboratory: an aneroid isoperibol calorimeter, [32,33] and a high temperature direct reaction calorimeter working up to 1000°C [34].

Most of calorimetric alloys were prepared directly in the high temperature reaction calorimeter. Pellets of the mixed powders weighing about 0.7 g were sealed in tantalum crucible under an argon atmosphere and dropped from a room temperature thermostat into the high temperature calorimeter. The calorimeter temperature was set at a value included between 650 and 900°C, according to the composition of the samples. Each sample was dropped twice

Table 1
Crystallographic data for the elements and the intermediate phases of the Sm–Ni system

Phase	Composition at.%Ni	Structure type	Lattice constants, *pm*			Ref.
			a	*b*	*c*	
(γ Sm)	0	*cI2* – W	≈410			[14]
(β Sm)	0	*hP2* – Mg	366.30		584.48	[14]
(α Sm)	0	*hR9* – α Sm[a]	362.90		2620.7	[14]
Sm_3Ni	25.0	*oP16* – Fe_3C	699	972	637	[15]
SmNi	50.0	*oC8* – CrB	377.6	1035.8	429.1	[16]
			377.2	1034.1	427.0	[17]
			373	1023	426	[18]
$SmNi_2$	66.7	*cF24* – Cu_2Mg	722.6			[19]
		HT form	722			[20]
			723.27			[21]
$Sm_{1-x}Ni_2$		Laves superstructure ordered vacancies in the Sm sites	Doubled cell parameter			[22]
$x \leq 0.05$		LT form				
$SmNi_3$	75.0	*hR36* – Be_3Nb[a]	500.5		2469	[23]
			500.3		2459	[24]
Sm_2Ni_7	77.8	*hP36* – Ce_2Ni_7 HT form	496.9		2435	[23]
		hR54 – Er_2Co_7[a] LT form	496.9		3653	[23]
Sm_5Ni_{19}	79.2	Sm_5Ni_{19}-polytypes	500		≈n×1600 (n=4, 6, 9, 12)	[25]
$SmNi_5$	83.3	*hP6* – $CaCu_5$	493		397	[20]
			492.4		397.4	[26]
Sm_2Ni_{17}	89.5	*hP38* – Th_2Ni_{17}	847.1		804.9	[27]
(Ni)	100	*cF4* – Cu	352.40			[28]

[a] The number of atoms in the, triple-primitive, hexagonal unit cell are indicated.

into the calorimeter from the room temperature thermostat. In the first run (reaction run) a mixture of the pure Sm and Ni metals is dropped; in the second, reference run, the synthesized alloy is used. In each run the calorimeter is calibrated with a procedure consisting in dropping four weighed silver spheres, two before and two after the alloy. The enthalpy of formation at room temperature of the alloy is obtained as the difference of the thermal effects observed in the reaction and reference runs.

With the aim of evaluating the error deriving from a possible not complete or not well-defined reaction, in several cases, 'reference' samples with the same composition, prepared by conventional techniques and proved to be in equilibrium, were used in the second drop step.

A few calorimetric samples were synthesized in another calorimeter [32,33], maintained in a water ultrathermostat at 27±0.01°C. In this case too, the formation heats were considered measured at 300 K because the sample in the calorimeter cooled down to this temperature during the measurement. This calorimeter consists of a thick aluminium cylinder containing two small electric furnaces, which are used for starting the reaction in the sample and for electric calibration, respectively. The sample (about 10–15 g) is a mixture of fine metal powders enclosed in a gas-tight inox crucible sealed by electric welding which is then inserted in the calorimeter and, after thermal equilibration, heated until the reaction starts. The temperature of the calorimeter is followed by a multiple-junction thermopile (differentially connected to the similar thermopile of another calorimeter which is identical to the first and used as a reference). The electric energy fed to the calorimeter in the reaction run and in the subsequent calibration runs is measured by means of a PC controlled acquisition system.

In order to check whether the equilibrium state had been reached and with respect to side reactions, the different samples prepared in the calorimeter, as those used as 'reference alloys', were studied by X-ray powder diffraction, optical and electron microscopy and electron probe microanalysis.

The X-ray analysis of the various alloys was carried out by the Debye method and by powder diffractometry using Cu and FeKα radiations. Powder photographs were used both for phase analysis and identification and for lattice parameter measurements. Metallographic examination was carried out after SiC paper, diamant paste polishing and after etching in air or in dilute alcoholic HNO_3 solution.

During this study both calorimetric and reference samples prepared with conventional techniques in the Sm_3Ni–SmNi region showed the presence of a new phase near to 37.0–40.0 at.%Ni stoichiometry. From our preliminary studies, however, it cannot be excluded that this phase is not stable at room temperature, but decomposes at a temperature below the eutectic one.

A thorough investigation of the phase diagram in the composition range 15–45 at.%Ni has been started by using differential scanning calorimetry, in order to have a better definition of the equilibria involved in this region.

As for the enthalpy of formation for the solid alloys at 300 K, no significant data have been obtained for this phase.

4. Results and discussion

The results obtained in the measurements of the heats of formation are listed in Table 2. A few data corresponding to alloys for which the reaction was incomplete have also been reported as an indication of the limits of the true $\Delta_f H$ values. The data corresponding to samples which reached the equilibrium state, together with those of the literature, were used to trace the trend of the $\Delta_f H$ vs. composition (Fig. 1) and to evaluate the most probable values of the standard enthalpies of formation for the different compounds. These values are also reported in Table 2.

We may notice a good agreement between the results so far obtained for the enthalpies of formation for the Sm–Ni solid alloys and the literature data. In particular the $\Delta_f H$ trend as a function of composition fit well the enthalpy values previously suggested or measured for the $SmNi_2$, $SmNi_5$ phases.

The trend of these values is characterized by a minimum in the $\Delta_f H°$ close to the $SmNi_2$–$SmNi_3$ composition, and shows slight discontinuities for the other intermediate compounds.

Table 2
Heats of formation of solid Sm–Ni alloys[a]

Nominal composition x_{Ni}	$-\Delta_f H°$ at 300 K kJ/mol at.	Remarks	Working T in the HT calorimeter °C
0.25	21.0	Aneroid calorimeter	–
0.32	24.5	HT calorimeter	655
0.32	25.0[b]	HT calorimeter	655
0.37	29.4	HT calorimeter	834
0.40	27.6	HT calorimeter	821
0.45	30.5	HT calorimeter	833
0.51	32.5	HT calorimeter	679
0.51	32.0	HT calorimeter	780
0.53_5	33.1[b]	HT calorimeter	907
0.54	33.3	HT calorimeter	770
0.60	(30.0)[c]	HT calorimeter	800
0.62	33.6	HT calorimeter	827
0.66_7	36.2	aneroid calorimeter	–
0.66_7	(31.2)[c]	HT calorimeter	679
0.68	35.4	HT calorimeter	810
0.74	(31.0)[c]	HT calorimeter	811

[a] Calorimetric data at 300 K for the reaction: $(1-x)\alpha Sm_{(solid)} + xNi_{(solid)} = Sm_{(1-x)}Ni_{x(solid)}$. Interpolated values of the $\Delta_f H°$ (kJ/mol of atoms) for the compounds: Sm_3Ni – 21.5±2; SmNi – 33.0;±1; and $SmNi_2$ – 36.0±1.

[b] Value obtained by comparison of the reaction sample with a reference sample (see text).

[c] For these alloys, the reaction in the calorimeter was not complete.

As a concluding remark on the thermochemistry of these alloys, a comparison with the literature data available for other isostructural rare earth–nickel compounds may be noteworthy. Several discrepancies may be noticed for specific compounds. Considering, for instance, the RNi_2 phase, the following data have been reported for the light rare earth metals, $\Delta_f H°$ (kJ/mol of atoms at 300 K, if not otherwise indicated): $LaNi_2$: −29.6 (emf, [35]), −20.4 (acid sol.cal., [36]), −33.8 (estimated [8]), $LaNi_{2.28}$: −41.9 (973 K, emf, [37,38]); $CeNi_2$: −38.6 (Al sol. cal., [39]); $PrNi_2$: −39.1 (973 K, emf, [37,38]); $SmNi_2$: −36.0 (dir. cal., this work), −37.7 (estimated, [8]), −34.5 (apparently evaluated from thermochemistry of hydrogenation reactions [9]).

In conclusion, we may remark that these data are in agreement with the exothermicity generally observed for the R alloys with the elements of the 10th group even if they are not so high as with the heavier Pd and Pt elements.

Acknowledgements

Planning and development of the studies here presented form a part of an Italian National Research Project entitled ‘Leghe e composti intermetallici. Stabilità termodinamica, proprietà fisiche e reattività’. The authors would like to thank the Italian Ministero dell’ Università e della Ricerca Scientifica e Tecnologica (Programmi di Ricerca Scientifica di Rilevante Interesse Nazionale) for financial support. Partial financial support has also been obtained from the Italian Consiglio Nazionale delle Ricerche under the ‘Progetto Finalizzato Materiali Speciali per Tecnologie Avanzate II’.

References

[1] T. Sakai, M. Matsuoka, C. Iwakura, in: K.A. Gschneidner Jr., L. Eyring (Eds.), Handbook on the Physics and Chemistry of Rare Earths, Vol. 21, North-Holland, Elsevier Science Publishers B.V, The Netherlands, 1995, p. 133.
[2] G. Borzone, N. Parodi, R. Ferro, in: Y.A. Chang, F. Sommer (Eds.), Thermodynamics of Alloy Formation, The Minerals, Metals, Materials Society, OH, USA, 1997, p. 59.
[3] R. Raggio, G. Borzone, R. Ferro, Intermetallics 8 (2000) 247.
[4] G. Borzone, N. Parodi, R. Raggio, R. Ferro, Proceedings of the XXVII Congresso di Chimica Inorganica, O8, Como, Italy, 1999.
[5] Y.Y. Pan, C.S. Cheng, Acta Phys. Sinica (China) 32 (1) (1983) 92.
[6] Y.Y. Pan, P. Nash, in: P. Nash (Ed.), Phase Diagrams of Binary Nickel Alloys, ASM International, Materials Park, OH, USA, 1991, p. 307.
[7] X. Li, Z. Wang, G. Liu, W. Zhan, S. Pan, Proceedings of the 6th National Symposium on Phase Diagrams, 1990, p. 125, Shenyang, China (quoted in Red Books Phase Diagrams of Metallic Systems, Vol. 35, VINITI and MSI, Stuttgart, Germany, 1990, p. 303).

[8] A.L. Shilov, Russ. J. Phys. Chem. 61 (1987) 719.

[9] R.A. Sirotina, Thesis, Moscow State University, Moscow, Russia, 1985.

[10] A. Pasturel, C. Colinet, P. Hicter, Phys. Status Solidi B 125 (1) (1984) 101–106.

[11] Q. Guo, O.J. Kleppa, Metall. Mater. Trans. B 29 (1998) 815.

[12] I.V. Nikolaenko, J. Alloys Comp. 225 (1995) 474.

[13] X. Su, W. Zhang, Z. Du, J. Alloys Comp. 278 (1998) 182.

[14] K.A. Gschneidner Jr., in: K.A. Gschneidner Jr., L. Eyring (Eds.), Handbook on the Physics and Chemistry of Rare Earths, Cumulative Index, Vols. 1–15, North-Holland, Elsevier Science Publishers B.V, The Netherlands, 1993, p. 509.

[15] R. Lemarie, D. Paccard, Bull. Soc. Fr. Min. Cristallogr. 90 (1967) 311.

[16] A.E. Dwight, R.A. Conner Jr., J.W. Downey, Acta Crystallogr. 18 (1965) 835.

[17] S.C. Abrahamans, J.L. Bernstein, R.C. Sherwood, J.H. Wernick, H.J. Williams, J. Phys. Chem. Solids 25 (1964) 1069.

[18] R.E. Walline, W.E. Wallace, J. Chem. Phys. 41 (6) (1964) 1587.

[19] J.H. Wernick, S. Geller, Trans. AIME 218 (1960) 866.

[20] K. Nassau, L.V. Cherry, W.E. Wallace, J. Phys. Chem. Solids 16 (1960) 123.

[21] R.C. Mansey, G.V. Raynor, I.R. Harris, J. Less-Common Met. 14 (1968) 329.

[22] E. Gratz, A. Kottar, A. Lindbaum, M. Mantler, M. Latroche, V. Paul-Boncour, M. Acet, Cl. Barner, W.B. Holzapfel, V. Pacheco, K. Yvon, J. Phys.: Condens. Matter. 8 (1996) 8351.

[23] K.H.J. Buschow, A.S. Van Der Goot, J. Less-Common Met. 221 (1970) 419.

[24] A.V. Virkar, A. Raman, J. Less-Common Met. 18 (1969) 59.

[25] S. Takeda, Y. Kitano, Y. Komura, J. Less-Common Met. 84 (1982) 317.

[26] S.E. Haszko, Trans. AIME 218 (1960) 763.

[27] K.H.J. Buschow, J. Less-Common Met. 11 (1966) 204.

[28] T.B. Massalski et al. (Eds.), Binary Alloy Phase Diagrams, Vols. 1–3, 2nd Edition, Metals Park, OH, USA, 1990.

[29] V. Paul-Boncour, C. Lartigue, A. Percheron-Guégan, J.C. Achard, J. Pannetier, J. Less-Common Met. 143 (1988) 301.

[30] A.V. Klimyenko, J. Seuntjens, L.L. Miller, B.J. Beaudry, R.A. Jacobson, K.A. Gschneidner Jr., J. Less-Common Met. 144 (1988) 133.

[31] H. Horikoshi, S. Takeda, Y. Komura, Jpn. J. Appl. Phys. 24 (1985) L210.

[32] R. Capelli, R. Ferro, A. Borsese, Thermochim. Acta 10 (1974) 13.

[33] R. Ferro, G. Borzone, N. Parodi, G. Cacciamani, J. Phase Equil. 15 (1994) 317.

[34] G. Cacciamani, G. Borzone, R. Ferro, J. Alloys Comp. 220 (1995) 106.

[35] T.N. Rezukhina, S.V. Kutsev, Zh. Fiz. Khim. 56 (1982) 1.

[36] K.N. Semenenko, R.A. Sirotina, A.P. Savchenkova, Zh. Fiz. Khim. 53 (1979) 2373.

[37] J. Dischinger, Thesis, Kiel University, Germany, 2000.

[38] J. Dischinger, H.-J. Schaller, J. Alloys Comp. 312 (2000) 201–210.

[39] B.P. Reddy, R. Baku, K. Nagarajan, V.R. Vasudeva Rao, J. Nucl. Mater. 247 (1997) 235.